Contact strength of ceramic laminates

Luca Ceseracciu, Emilio Jiménez-Piqué, Theo Fett, Marc Anglada

Contact strength of ceramic laminates

Luca Ceseracciu, Emilio Jiménez-Piqué, Theo Fett, Marc Anglada

PII: S0266-3538(07)00205-9
DOI: 10.1016/j.compscitech.2007.04.020
Reference: CSTE 3706

To appear in: *Composites Science and Technology*

Received Date: 30 March 2007
Revised Date: 24 April 2007
Accepted Date: 30 April 2007

Please cite this article as: Ceseracciu, L., Jiménez-Piqué, E., Fett, T., Anglada, M., Contact strength of ceramic laminates, *Composites Science and Technology* (2007), doi: 10.1016/j.compscitech.2007.04.020

Contact strength of ceramic laminates

Luca Ceseracciu [a,*] Emilio Jiménez-Piqué [a] Theo Fett [b]
Marc Anglada [a]

[a] *Departament de Ciència dels Materials i Enginyeria Metal·lúrgica, Universitat Politècnica de Catalunya, Av. Diagonal 647, 08028 Barcelona, Spain*

[b] *Institut für Keramik im Maschinenbau, University of Karlsruhe, 7 Haid-und-Neu-Straße, 76131 Karlsruhe, Germany*

Abstract

Ceramic laminates with residual stress arising from thermal mismatch, show higher strength and larger apparent fracture toughness than their monolithic counterparts. For an effective improvement under in-service conditions, such enhancement should be reflected on the blunt-contact behaviour, characterized by an inhomogeneous multiaxial stress state.

The contact strength test is an interesting alternative to traditional testing methods to evaluate contact-focused resistance of brittle materials. Because of the Hertzian-like stress state, high stresses can be generated far from the surface, producing failure from the weakest part of the structure, and this is especially true in pre-stressed materials, such as the one herein studied.

In this work, experimental tests on a laminated ceramic are reported together with a FE analysis, showing a noteworthy improvement, although in some cases the composite structure may fail in an inner layer, and providing general tools for designing contact-resistant structures.

Key words: A. Layered structures, B. Contact strength, C. Finite element analysis (FEA), C. Residual stresses

1 Introduction

Intrinsic brittleness and lack of reliability are the main limitations to the extended use of ceramic materials in advanced applications, in which their

* Corresponding author. Tel.: +34934054452; Fax.: +34934016706
Email address: luca.ceseracciu@upc.edu (Luca Ceseracciu).

exceptional properties, such as wear and chemical resistance, hardness, or low friction coefficient, are required. Laminated structures [1] are one of the routes pursued in order to improve the fracture resistance and/or reliability of ceramic materials. Laminates have been produced that take advantage of several strengthening mechanisms, such as crack deflection [2], independence on the initial flaw, producing threshold strength [3], or weak interfaces increasing the work of fracture causing thus "graceful failure" [4].

Among them, one of the most common mechanisms is the incorporation of residual stresses arising from thermal expansion coefficients mismatch, so that the surface layer (usually some hundred micrometers thick) is under compression, and the effective stress is reduced, as well as stress intensity factors [5]. The effectiveness of such a mechanism has been proved under conventional bending strength tests [6,7]. The stress produced by such test is with good approximation uniaxial and presents a small stress gradient; for this reason it is widely used for strength characterization of brittle materials, such as advanced ceramics. However, more realistic loading involve multiaxial inhomogeneous stress fields, rather than uniaxial homogeneous stress states[8]. Laminates have shown superior mechanical properties than the monolithic counterparts, for example, in wear tests [9] and localized blunt loading (spherical indentation) [10]. These tests are focused on surface damage, but even though they describe resistance to surface degradation, which leads to functionality loss, they are not completely appropriate for a global evaluation of a surface-related strength, even under severe conditions [11].

Among the alternative tests proposed for a strength characterization focused on contact-prone applications, the contact strength test is particularly simple and material inexpensive. Compression applied by two opposite cylinders produces a Hertzian stress field, with the first in-plane principal stresses tensile and the second negative, the former presenting maxima at the surface near the contact zone and along the vertical axis of symmetry, which causes unstable crack growth and failure of the sample. The stress field was computed numerically by Fett *et al.* [12], who established the simple relation

$$\sigma_x^{max} = 0.490\sigma^* \tag{1}$$

for point-load, with $\sigma^* = P/Ht$, normalized load, t the sample width and the other symbols as in Fig. 1. Under pressure load in a contact zone of width s, expressed with the Hertzian pressure distribution $p(x) = p_0\sqrt{1-(2x/s)^2}$, the maximum stress is slightly reduced, no more than 1%, as s increases. Tensile stress is generated also along the symmetry axis; eq.1 is valid under point-load, with the maximum located on the loading point; however, if the contact zone is non-singular, the ratio σ_x^{max}/σ^* drops down rapidly as s

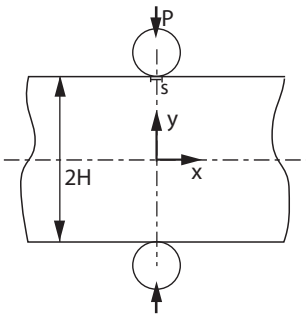

Fig. 1. Scheme of the contact strength test: parallel strip subjected to compression by opposite rigid cylinders.

increases, so that fracture is normally expected on the surface rather than within the material.

Experimental results of contact strength tests showed strength values in agreement with those from bending tests, while Weibull exponents were roughly halved [12]. This latter is due to the high stress gradient generated [13] and should not be seen as a limitation of the method, but rather as an indication of how dangerous multiaxial contact loading can be and that a specific testing methodology is recommended, whenever such a type of loading is expected *in-service*. This is the case of ceramic multilayers, whose main application are related to surface resistance, and have not been studied, as yet, by the point of view of contact strength.

In this work contact strength tests were performed on an alumina-based laminated material and compared with monolithic alumina produced in a similar way, as explained below. Bidimensional Finite Elements models were developed to study the interaction of the complex Hertzian field with the residual stresses in the laminates and provide a tool for design of contact resistant laminates.

2 Materials and experimental procedure

Layers of pure alumina and 60% alumina-40% zirconia were produced at ISTEC (Faenza, Italy) with the tape casting technique, starting from high-purity alumina powders (Alcoa A16-SG, Alcoa Aluminum Co., New York, NY). A multilayer structure, showed in Fig. 2, was produced by alternate stacking of 13 layers of the two materials, and sintering at 1550°C, with final layer thickness of approx. 200 μm and residual stresses of approx. $\sigma_r = -200MPa$ in the alumina layers and $\sigma_r = 200MPa$ in the alumina-zirconia layers. Alumina layers were stacked and sintered in order to obtain a monolithic material with microstructure similar to the laminate (approx. 2 μm-sized grains). Further details on the processing are reported

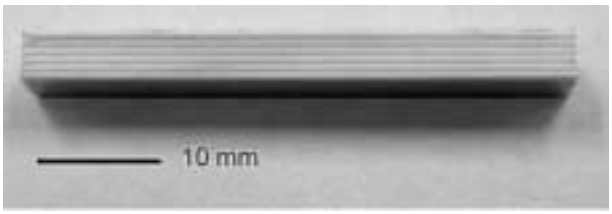

Fig. 2. Optical micrograph of alumina-based laminated structure. The darker layers are made of alumina, the lighter ones of alumina-zirconia

elsewhere [9].

Contact strength tests were performed on an universal testing machine. Samples were placed with the external, compressive layer in contact with the rollers. Load was applied by two opposite $4mm$ radius hardened steel rollers at the constant rate of 100 N/s. The rate chosen is slightly lower than suggested for strength tests, in order to better identify, with visual aid, the fracture load, as mentioned below; however, no subcritical crack growth is expected under this kind of test [14]. Tests were interrupted when fracture occurred, with either or both extremities of the sample falling apart, and often the remaining portion shattering for compression. Fracture loads were recorded and the critical load for the first fracture event, sometimes coinciding with the ultimate strength, sometimes with an earlier pop-in.

3 Finite Element Model

For a better understanding of the behaviour of laminated structures, a Finite Elements model was developed and first verified by simulating testing of monolithic materials. One quarter of a bar, whose geometry and size were taken from actual samples, was represented on a bidimensional model. A coding script was created in the Python built-in language to allow automatic generation of any symmetrical odd-layered structure, given the layers number and thickness.

The models of the systems studied consisted of a mesh of approx. 25000 quadratic elements, established after mesh convergence tests, refined at the contact zone, where higher stress gradient was expected. The length of the bars was three times the thickness, guaranteeing negligible influence of the free boundary to the stress field [12]. The rollers were represented with a rigid analytical body, applying a progressive displacement on the bar surface. The corresponding load was calculated from the reaction forces at the roller. A step of shrinkage was included for generating the residual stresses in the laminated structures, starting from the temperature of 1200°C, above which

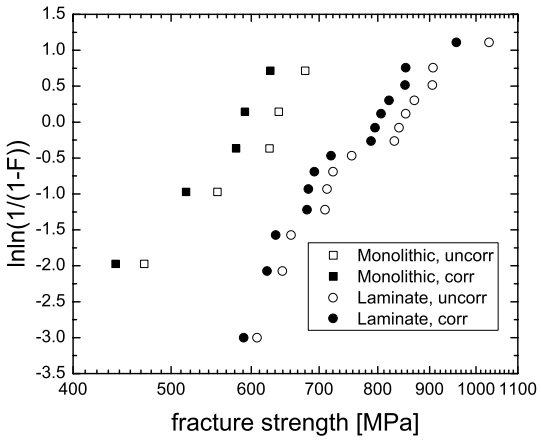

Fig. 3. Weibull plot of the contact strength of monolithic alumina and alumina/alumina-zirconia multilayer. Values from numerical (empty symbols) and Finite Elements (solid symbols) solutions are presented.

zirconia behave as plastic and therefore no stress is generated [15], to room temperature (30°C).

4 Results and Discussion

4.1 Experimental results

Experimental results for monolithic and laminated materials, respectively, are presented as a Weibull plot of the probability of failure F in Fig. 3, both as calculated from eq.1 and with the correction function discussed below (section 4.2).

Although the number of pure alumina sample tested is not high enough for a proper statistical analysis of the former material, the Weibull exponent m (11, with the 90% confidence interval [4.0; 16.1]) calculated by the "Maximum Likelihood Procedure" confirmed previously reported values [12], and the strength ($625MPa$ [563; 703] and $579MPa$ [524; 648] from numerical and FE expression, respectively) is in agreement with values for fine-grained alumina.

The numerical and FE values do not differ significantly, being the dispersion within the experimental error; it is thought, therefore, that the simpler approach can be considered valid, as long as no major accuracy is needed. The strength of the laminate was found of $840MPa$ [781; 904] and $794MPa$

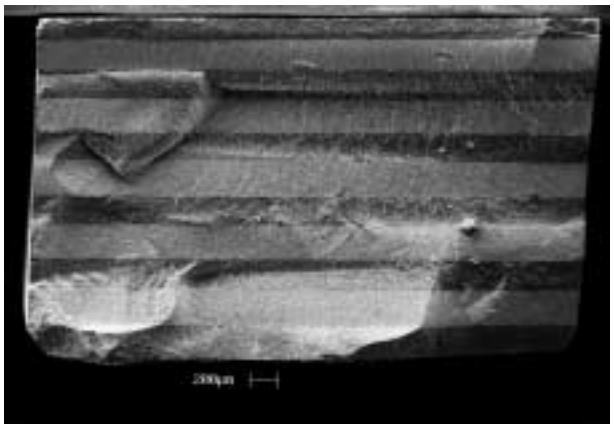

Fig. 4. Electron Fractography of tested multilayer sample, showing that fracture started from the alumina surface layer.

[744; 849] from numerical and FE expression, respectively.

The values measured in this case relate to an effective strength of the structure, rather than to intrinsic strength of the material. Consistently, the improvement respect to monolithic material coincides with the amount of residual stresses, as confirmed by FE analysis. The micrograph in Fig. 4 shows that fracture started from the surface, as in the rest of specimens.

4.2 Finite Element

Finite Elements calculations in monolithic alumina showed that, respect to the numerical solutions, a slightly higher variation of the maximum stress was found with the increment of contact zone width s, reaching values approx. 10% lower in the considered range. This is attributed to the relatively high deformation the material is subjected to, and that is taken into account in the FE simulation, since the rollers are represented as rigid bodies, and not in the previous numerical. This different approach changes slightly the calculation of the stress field, with increasing weight as s grows.

A polynomial correction curve was defined as a function of normalized contact zone s/H, in the formulation:

$$\frac{\sigma_x^{max}}{\sigma^*} \equiv Y = Y_0 - a\left(\frac{s}{H}\right) - b\left(\frac{s}{H}\right)^2 \tag{2}$$

For an easier application to the experimental results in the specific case, another relation was extracted for the specific case as a function of the

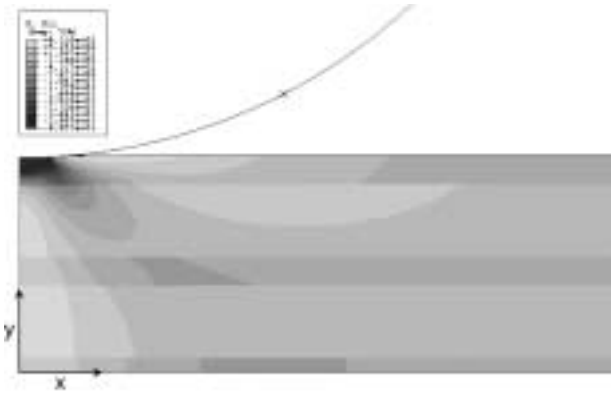

Fig. 5. Typical x-direction stress field in multilayer material, originated from the combination of residual stresses and testing stress fields

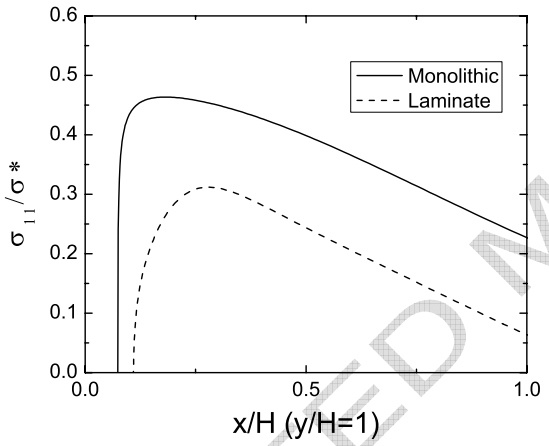

Fig. 6. Normalized tensile stress in the surface of monolithic alumina and multilayer. The difference in the maximum values coincides with the compressive residual stress in the latter.

normalized load σ^*:

$$Y = Y_0 - a'\sqrt{\sigma^*} - b'\sigma^* \tag{3}$$

With Y_0 being the point-load value 0.489, and $a = 0.312$, $b = 0.25$, $a' = 1.3 \cdot 10^{-3}$, $b' = 4 \cdot 10^{-6}$ fitting parameters (for σ^* in MPa).
The difference with the $Y = constant$ solution is not substantial and could be neglected, however it should be noticed that the former solution slightly overestimates the strength of the material, reducing thus the safety factor. In the next section both the numerical and FE values are presented and compared.

Simulations of testing of the laminated material showed that the difference in terms of tensile stress, as could be expected, corresponds to the amount of residual stress. Apart from that, and a slight shift of the point of maximum stress shown in Fig. 6, no substantial difference was found, so that the relation 2 can be expressed in a form that includes the residual stress σ_r, leading to:

$$\sigma - \sigma_r = \left(Y_0 - a\left(\frac{s}{H}\right) - b\left(\frac{s}{H}\right)^2\right)\sigma^* \tag{4}$$

The shape of the correction curve depends slightly on the geometry and materials of the laminated structure and on the rollers radius; for higher accuracy it can be obtained specifically for any case studied.
Similar correction curves can be obtained for the maximum stress along the y-direction; in this case the best fit was obtained with the relation:

$$Y = Y_0 - a''\sqrt{\frac{s}{H}} - b''\frac{s}{H} \tag{5}$$

with $a'' = 0.8024$, $b'' = 0.5969$.

It can be noticed from eq. 5 that along the y-axis, as the contact zone increases, the relative stress is reduced with a much higher rate than on the surface. It can be expected therefore, considering also the likely presence of surface flaws, that fracture is more probable to start at the surface. In the case of laminated materials, in contrast with the monolithic case, the combination of residual and applied stress fields on the inner tensile layers of laminates can reach tensile values higher than the corresponding surface stress. Tensile stresses along the y-axis for monolithic and laminated material are reported in Fig. 7 for two arbitrary values of σ^*. The contribution from residual stresses is constant; therefore, under a low load, such a contribution is significant, leading, in the presented case, to a double total value with respect to that on the surface ($\sigma_x^{max} \approx \sigma^*$), while under a higher load, the same constant value sums to a value of relative applied stress which is lower ($\sigma_x^{max} \approx 0.3\sigma^*$), for the decrement explained above with the correction curve (eq. 5), so that, despite of the presence of the additional contribution, the total stress is lower than on the surface.

The global behaviour is summarized in Fig. 8, where the maximum stress along the surface and the y-axis, respectively, of the laminated structure is plotted against the normalized load σ^*. A critical value σ_c^* can be defined, below which stress is higher on the y-axis, and above which it is higher on the surface.

It should be noticed that the graphic above presented does not allow

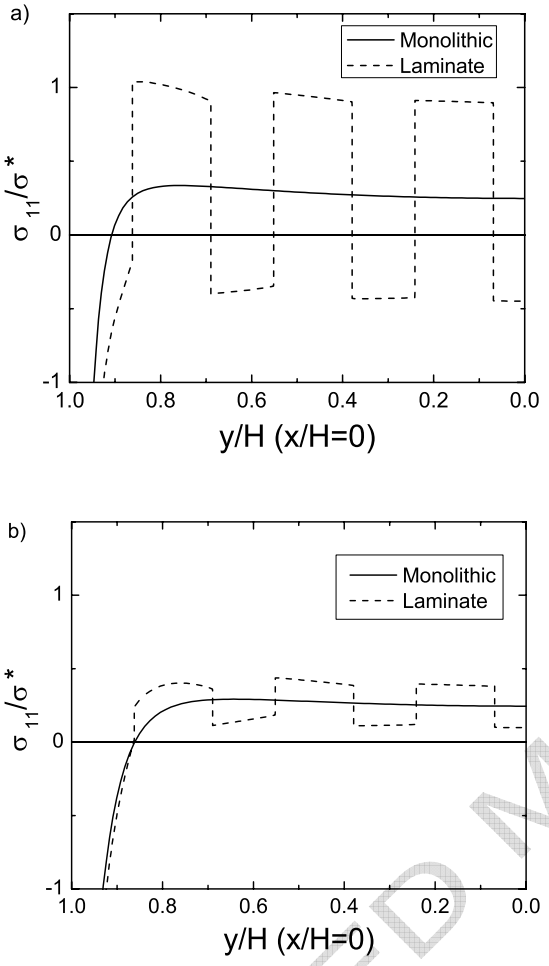

Fig. 7. Tensile stress along the y-axis ($x/H = 0$) for monolithic and laminated materials under low load, a) and high load b).

prediction of the fracture location, unless the strength of both composing materials is known, as well as the flaw distribution. It points out, nevertheless, that fracture could occur on other location than the surface; therefore, when fracture load is near the critical value σ_c^*, strength tests should be coupled with micrographic evaluation of the fracture location for a correct understanding of the failure.

In the case presented in this study (section 4.1), for example, the average strength measured coincides with a maximum stress located on the y-axis. Nevertheless, fractography observation, as in Fig. 4, showed that fracture started from the outer, compressive, layer.

Such a behaviour can be explained with a different strength of the composing materials, due to the smaller grain size in presence of ZrO_2, which acts as a

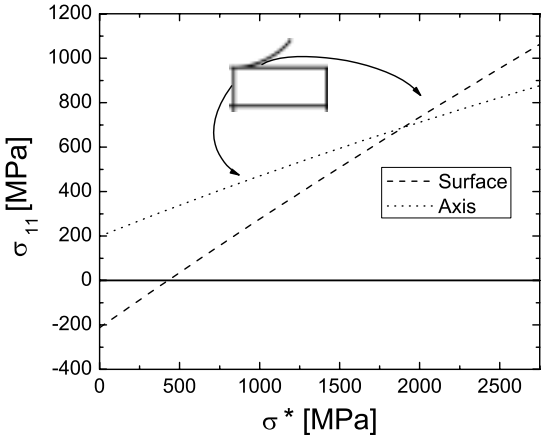

Fig. 8. Maximum tensile stress along the surface ($y/H = 1$) and the y-axis ($x/H = 0$) for multilayer material as a function of normalized load σ^*. The scheme indicates the approximate locations of the maximum stresses.

constraint to the grain growth [16], decreasing thus the initial flaw size, or to the higher amount of defects in the surface than in the bulk material.

The correct evaluation of the site of fracture initiation, combined with the calculated normalized load, as in Fig. 8, allows one to determine the resistance of the laminated structure, and also the strength of one, typically the weakest, of the composing materials, giving moreover information of a lower limit to the strength of the other. Alternatively, if the equivalent strength of a laminated structure is compared with tests on similar, unstressed, materials, as in the example below, an estimation of the residual stresses can be obtained.

Another interesting consideration derived from Fig. 8 is that under low normalized load σ^*, the stress on an internal layer of the laminate is higher than on the corresponding monolithic material. If the fracture strength is located in this first range, which is a condition that depends both on the laminated composing materials and geometry, the contribution of the residual stress to the strengthening would result detrimental, instead of beneficial, to the contact strength.

The maximum stress presented in Fig. 8 was plotted for a specific laminate. Changes of the geometry and/or of the composing materials influence the global behaviour. As a good approximation, the $\sigma_x^{max} \quad vs \quad \sigma^*$ relations, both on the surface and on the axis, as in fig. 8 in presence of residual stress are just shifted from the origin along the y-axis to the respective value of stress. The critical (normalized) load for change of maximum location is shown on Fig. 8, where it can be seen that the choice of the composing

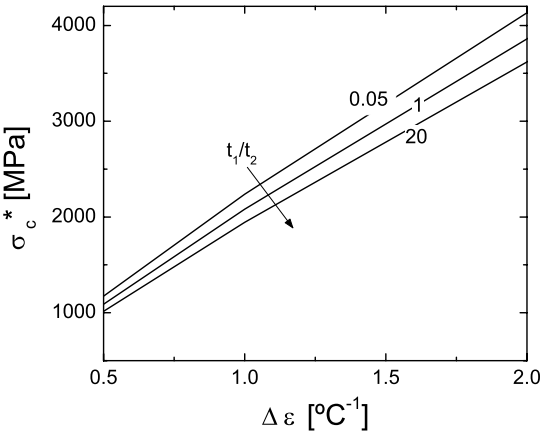

Fig. 9. Influence of the thermal mismatch and of the tensile versus compressive stress ratio (labelled as t_1/t_2)on the critical normalized load σ_c^* for the switching of the maximum location from y-axis to surface, on laminated materials.

materials, especially the thermal expansion mismatch, has the greatest influence on the critical load; while such value varies only slightly as the laminated structure, *i.e.* the tensile/compressive stresses ratio, changes.

The general information that can be extracted is that extensive thermal mismatch should be avoided in the laminated design; and that, expectedly enough, higher compressive stresses provide higher contact resistance and lower susceptibility to abnormal internal fracture. Since the location of the maximum stress on the axis changes, displacing deeper into the material as the contact zone increases, it is possible that the "unstressed" maximum, which is the σ_x stress minus the residual stresses, is located on a compressive layer. In that case, the real maximum value is lower than showed on Fig 8. This effect is not predictable *a priori* unless information of the range of fracture stress and of the laminate geometry is provided.

5 Conclusions

The contact strength test is an effective method for characterizing advanced ceramic materials with a simple experimental setup, yet well representative of in-service loading conditions of many applications.

Contact strength of an alumina-based laminated structure was evaluated with such a test, showing a noteworthy improvement of strength, corresponding to the compressive residual stresses present in the external layer.

Despite of this, expectable, result, Finite Elements analysis of the test indicated that high stress can be reached in the interior of the sample, corresponding to the tensile layers, suggesting the possibility of failure for load lower than predicted and even lower than the strength of the monolithic counterpart, depending on the composing materials (in terms of thermal mismatch and relative strength) and on the geometry of the laminate.

In general terms, design of ceramic laminated structure should always be based on the type of loading expected in service, in order to avoid undesired stress amplifications that could make ineffective, or even detrimental, the extrinsic strengthening.

Acknowledgments

Work supported in part by the Spanish Ministry of Science and Education through grant MAT-2006-1348C02-02.
L.C. acknowledges the Spanish Ministry of Science for funding through grant AP-2004-0475.
The authors wish to thank Dr. Oberacker and Dr. Pascual for fruitful discussion.

References

[1] Chan HM. Layered ceramics: Processing and mechanical behavior. Annu Rev Mater Sci 1997;27:249–282.

[2] Prakash O, Sarkar P, Nicholson PS. Crack deflection in ceramic/ceramic laminates with strong interfaces. J Am Ceram Soc 1995;78(4):1125–7

[3] Bermejo R Torres Y, Sanchez-Herencia AJ, Baudin C, Anglada M, Llanes L. Residual stresses, strength and toughness of laminates with different layer thickness ratios Acta Mater 2006;54(18):4745–4757

[4] Clegg WJ, Kendall K, Alford N McN, Button TW, Birchall JD. Simple way to make tough ceramics. Nature 1990;347(6292):445–457

[5] de Portu G, Micele L, Pezzotti G. Laminated ceramic structures from oxide systems. Composites Part B 2006;37:556–567.

[6] Hansen JJ, Cutler RA, Shetty DK, Virkar AV. Indentation Fracture Response and Damage Resistance of Al_2O_3-ZrO_2 Composites Strengthened by Transformation-Induced Residual Stresses. J Am Ceram Soc 1988;71(12):C501–5

[7] Chen CR, Pascual J, Fischer FD, Kolednik O, Danzer R. Prediction of the fracture toughness of a ceramic multilayer composite - Modeling and experiments. Acta Mater 2007;55(2):409–421.

[8] Pavon J, Jiménez-Piqué E, Anglada M, Saiz E, Tomsia AP. Monotonic and cyclic Hertzian fracture of a glass coating on titanium-based implants. Acta Mater 2006;54(13):3593–3603.

[9] Toschi F, Melandri C, Pinasco P, Roncari E, Guicciardi S, de Portu G. Influence of Residual Stresses on the Wear Behavior of Alumina/Alumina-Zirconia Laminated Composites. J Am Ceram Soc 2003;86(9):1547–1553.

[10] Jiménez-Piqué E, Ceseracciu L, Chalvet F, Anglada M, de Portu G. Hertzian contact fatigue on alumina/alumina-zirconia laminated composites. J Eur Ceram Soc 2005;25(15):3393–3401.

[11] Ceseracciu L, Chalvet F, de Portu G, Anglada M, Jiménez-Piqué E. Surface contact degradation of multilayer ceramics under cyclic subcritical loads and high number of cycles. Int J Refr & Hard Mat 2005;23(4–6):375–381.

[12] Fett T, Munz D, Thun G. Test devices for strength measurements of bars under contact loading. J Test Eval 2001;29(1):1–10.

[13] Fett T, Munz D. Influence of stress gradients on failure in contact strength tests with cylinder loading. Engng Fract Mech 2002;69:1353–1361.

[14] Fett T, Creek D, Badenheim D, Oberacker R. Crack growth data from dynamic tests under contact loading? J Eur Ceram Soc 2004;24:2049–2054.

[15] Hillman C, Suo Z, Lange FF. Cracking of laminates subjected to biaxial tensile stress. J Am Ceram Soc 1996;78(8):2127–2133

[16] Nagl MM, Llanes L, Fernández R, Anglada M. The fatigue behaviour of Mg-PSZ and ZTA ceramics. Fracture of Mechanics Vol. 12, Plenum Press, 1996 pp.61–76